Metalloporphyrin polymer with temporally agile, broadband nonlinear absorption for optical limiting in the near infrared

Joel M. Hales,[1] Matteo Cozzuol,[1] Thomas E. O. Screen,[2] Harry L. Anderson,[2] and Joseph W. Perry[1,*]

[1]*School of Chemistry and Biochemistry, Center for Organic Photonics and Electronics, Georgia Institute of Technology, 901 Atlantic Dr. NW, Atlanta, Georgia 30332, (U.S.A)*
[2]*Department of Chemistry, Chemistry Research Laboratory, University of Oxford, Oxford, OX1 3TA, (U.K.)*
[*]*joe.perry@chemistry.gatech.edu*

Abstract: A lead bis(ethynyl)porphyrin polymer possesses strong nonlinear absorption with unprecedented spectral/temporal coverage as a result of broad, overlapping two-photon and excited-state absorption bands with favorable excited-state dynamics. Consequently, this material exhibits effective optical limiting over a range of about 500 nm in the near infrared (ca. 1050 – 1600 nm) and for laser pulsewidths spanning from 75 fs to 40 ns. Introduction of the material in a waveguide device geometry results in a strong optical limiting response.

OCIS codes: (190.0190) Nonlinear optics; (190.4710) Optical nonlinearities in organic materials; (190.4180) Multiphoton processes; (190.7110) Ultrafast nonlinear optics; (070.4340) Nonlinear optical signal processing; (130.2790) Guided waves

References and Links

1. E. W. Van Stryland, H. Vanherzeele, M. A. Woodall, M. J. Soileau, A. L. Smirl, S. Guha, and T. F. Boggess, "2 photon-absorption, nonlinear refraction, and optical limiting in semiconductors," Opt. Eng. **24**, 613-623 (1985).
2. L. W. Tutt and A. Kost, "optical limiting performance of C-60 and C-70 solutions," Nature **356**, 225-226 (1992).
3. J. W. Perry, K. Mansour, I. Y. S. Lee, X. L. Wu, P. V. Bedworth, C. T. Chen, D. Ng, S. R. Marder, P. Miles, T. Wada, M. Tian, and H. Sasabe, "Organic optical limiter with a strong nonlinear absorptive response," Science **273**, 1533-1536 (1996).
4. G. S. He, L. X. Yuan, J. D. Bhawalkar, and P. N. Prasad, "Optical limiting, pulse reshaping, and stabilization with a nonlinear absorptive fiber system," Appl. Opt. **36**, 3387-3392 (1997).
5. M. R. E. Lamont, M. Rochette, D. J. Moss, and B. J. Eggleton, "Two-photon absorption effects on self-phase-modulation-based 2R optical regeneration," IEEE Photon. Technol. Lett. **18**, 1185-1187 (2006).
6. B. L. Justus, A. L. Huston, and A. J. Campillo, "Broad-band thermal optical limiter," Appl. Phys. Lett. **63**, 1483-1485 (1993).
7. K. Mansour, M. J. Soileau, and E. W. Vanstryland, "Nonlinear optical-properties of carbon-black suspensions (ink)," J. Opt. Soc. Am. B-Opt. Phys. **9**, 1100-1109 (1992).
8. X. Sun, R. Q. Yu, G. Q. Xu, T. S. A. Hor, and W. Ji, "Broadband optical limiting with multiwalled carbon nanotubes," Appl. Phys. Lett. **73**, 3632-3634 (1998).
9. P. A. Bouit, G. Wetzel, G. Berginc, B. Loiseaux, L. Toupet, P. Feneyrou, Y. Bretonniere, K. Kamada, O. Maury, and C. Andraud, "Near IR nonlinear absorbing chromophores with optical limiting properties at telecommunication wavelengths," Chem. Mater. **19**, 5325-5335 (2007).
10. J. Wang, Y. Hernandez, M. Lotya, J. N. Coleman, and W. J. Blau, "Broadband Nonlinear Optical Response of Graphene Dispersions," Adv. Mater. **21**, 2430-2435 (2009).
11. H. L. Anderson, S. J. Martin, and D. D. C. Bradley, "Synthesis and 3rd-order nonlinear-optical properties of a conjugated porphyrin polymer," Angew. Chem.-Int. Ed. Engl. **33**, 655-657 (1994).
12. F. C. Grozema, C. Houarner-Rassin, P. Prins, L. D. A. Siebbeles, and H. L. Anderson, "Supramolecular control of charge transport in molecular wires," J. Am. Chem. Soc. **129**, 13370-+ (2007).
13. J. R. G. Thorne, S. M. Kuebler, R. G. Denning, I. M. Blake, P. N. Taylor, and H. L. Anderson, "Degenerate four-wave mixing studies of butadiyne-linked conjugated porphyrin oligomers," Chem. Phys. **248**, 181-193 (1999).

#115474 - $15.00 USD Received 10 Aug 2009; revised 23 Sep 2009; accepted 24 Sep 2009; published 29 Sep 2009

14. M. O. Senge, M. Fazekas, E. G. A. Notaras, W. J. Blau, M. Zawadzka, O. B. Locos, and E. M. N. Mhuircheartaigh, "Nonlinear optical properties of porphyrins," Adv. Mater. **19**, 2737-2774 (2007).
15. M. Pawlicki, H. A. Collins, R. G. Denning, and H. L. Anderson, "Two-Photon Absorption and the Design of Two-Photon Dyes," Angew. Chem.-Int. Ed. **48**, 3244-3266 (2009).
16. K. S. Kim, J. M. Lim, A. Osuka, and D. Kim, "Various strategies for highly-efficient two-photon absorption in porphyrin arrays," J. Photochem. Photobiol. C-Photochem. Rev. **9**, 13-28 (2008).
17. M. Drobizhev, Y. Stepanenko, A. Rebane, C. J. Wilson, T. E. O. Screen, and H. L. Anderson, "Strong cooperative enhancement of two-photon absorption in double-strand conjugated porphyrin ladder arrays," J. Am. Chem. Soc. **128**, 12432-12433 (2006).
18. T. V. Duncan, K. Susumu, L. E. Sinks, and M. J. Therien, "Exceptional near-infrared fluorescence quantum yields and excited-state absorptivity of highly conjugated porphyrin arrays," J. Am. Chem. Soc. **128**, 9000-9001 (2006).
19. M. K. Kuimova, M. Hoffmann, M. U. Winters, M. Eng, M. Balaz, I. P. Clark, H. A. Collins, S. M. Tavender, C. J. Wilson, B. Albinsson, H. L. Anderson, A. W. Parker, and D. Phillips, "Determination of the triplet state energies of a series of conjugated porphyrin oligomers," Photochem. Photobiol. Sci. **6**, 675-682 (2007).
20. T. E. O. Screen, J. R. G. Thorne, R. G. Denning, D. G. Bucknall, and H. L. Anderson, "Two methods for amplifying the optical nonlinearity of a conjugated porphyrin polymer: transmetallation and self-assembly," J. Mater. Chem. **13**, 2796-2808 (2003).
21. J. W. Perry, K. Mansour, S. R. Marder, K. J. Perry, D. Alvarez, and I. Choong, "Enhanced reverse saturable absorption and optical limiting in heavy-atom-substituted phthalocyanines," Opt. Lett. **19**, 625-627 (1994).
22. K. J. Thorley, J. M. Hales, H. L. Anderson, and J. W. Perry, "Porphyrin dimer carbocations with strong near infrared absorption and third-order optical nonlinearity," Angew. Chem.-Int. Ed. **47**, 7095-7098 (2008).
23. R. L. Sutherland, M. C. Brant, J. Heinrichs, J. E. Rogers, J. E. Slagle, D. G. McLean, and P. A. Fleitz, "Excited-state characterization and effective three-photon absorption model of two-photon-induced excited-state absorption in organic push-pull charge-transfer chromophores," J. Opt. Soc. Am. B-Opt. Phys. **22**, 1939-1948 (2005).
24. T. V. Duncan, T. Ishizuka, and M. J. Therien, "Molecular engineering of intensely near-infrared absorbing excited states in highly conjugated oligo(porphinato)zinc-(polypyridyl)metal(II) supermolecules," J. Am. Chem. Soc. **129**, 9691-9703 (2007).
25. R. Bonneau, I. Carmichael, and G. L. Hug, "Molar Absorption-Coefficients of Transient Species in Solution," Pure Appl. Chem. **63**, 290-299 (1991).
26. A. Karotki, M. Drobizhev, M. Kruk, C. Spangler, E. Nickel, N. Mamardashvili, and A. Rebane, "Enhancement of two-photon absorption in tetrapyrrolic compounds," J. Opt. Soc. Am. B-Opt. Phys. **20**, 321-332 (2003).
27. I. C. Khoo, M. V. Wood, M. Lee, and B. D. Guenther, "Nonlinear liquid-crystal fiber structures for passive optical limiting of short laser pulses," Opt. Lett. **21**, 1625-1627 (1996).
28. J. J. Butler, S. R. Flom, J. S. Shirk, T. E. Taunay, B. M. Wright, and M. J. Wiggins, "Optical limiting properties of nonlinear multimode waveguide arrays," Opt. Express **17**, 804-809 (2009).
29. J. J. Butler, J. J. Wathen, S. R. Flom, R. G. S. Pong, and J. S. Shirk, "Optical limiting properties of nonlinear multimode waveguides," Opt. Lett. **28**, 1689-1691 (2003).
30. I. C. Khoo, A. Diaz, M. V. Wood, and P. H. Chen, "Passive optical limiting of picosecond-nanosecond laser pulses using highly nonlinear organic liquid cored fiber array," IEEE J. Sel. Top. Quantum Elec. **7**, 760-768 (2001).
31. G. E. OKeefe, J. J. M. Halls, C. A. Walsh, G. J. Denton, R. H. Friend, and H. L. Anderson, "Ultrafast field-induced dissociation of excitons in a conjugated porphyrin polymer," Chem. Phys. Lett. **276**, 78-83 (1997).

1. Introduction

Materials exhibiting optical limiting via strong nonlinear absorption (NLA) could provide a means to protect optical sensors from pulsed laser emission [1-3], for signal conditioning via dynamic noise suppression [4], and for optical signal regeneration [5]. The near infrared (NIR) spectral region (1000 – 1600 nm) is particularly important for all-optical signal processing since it includes the telecommunications bands and the wavelength of the ubiquitous, high-powered Nd:YAG laser (1064 nm). Unfortunately, the stringent conditions placed on NLA materials to exhibit effective optical limiting have hindered its widespread use. An ideal material for optical limiting should exhibit high transmittance at low input irradiances or fluences but be able to rapidly suppress intense, pulsed light prior to passing through the material; furthermore these characteristics should be maintained over a broad spectral and temporal dynamic range. This is a difficult task since most mechanisms typically employed for optical limiting, such as reverse saturable absorption (or one-photon induced excited-state absorption, 1PA-ESA) [2, 3], nonlinear refraction [6] and nonlinear scattering

#115474 - $15.00 USD Received 10 Aug 2009; revised 23 Sep 2009; accepted 24 Sep 2009; published 29 Sep 2009

[7], are most effective for pulsewidths of about 1 ns or longer. Reverse saturable absorption can be somewhat effective for shorter pulsewidths but has the additional restriction of a limited spectral range due to the presence of one-photon resonances near the excitation wavelength, leading to non-negligible linear absorption.

Consequently, while a few materials have exhibited effective optical limiting in the NIR spectral region [8-10], they have been restricted to narrow spectral regions and limited temporal dynamic range. Two-photon induced excited-state absorption (2PA-ESA) has the potential to overcome the latter constraint since optical transparency is intrinsically high for materials being excited by 2PA with photon energies below the material's energy bandedge. However, in order to achieve effective optical limiting the spectra associated with the 2PA and ESA must exhibit broad, overlapping bands and their two-photon and one-photon cross-sections must be sizable (i.e. $\delta > 1000 \times 10^{-50}$ cm^4 s photon^{-1} and $\sigma > 1 \times 10^{-20}$ m^2, respectively, per molecule), particularly for longer pulsewidths, since the excitation mechanism (2PA) is nonlinearly dependent on irradiance. Furthermore, for broad temporal dynamic range optical limiting, significant ESA contributions from states that are formed rapidly and states that are relatively long-lived (e.g. states in the singlet and triplet manifolds, respectively) must be present. Here, we report on a lead-based bis(ethynyl)porphyrin polymer that effectively combines extremely strong and broadband two-photon absorption (2PA) and excited-state absorption (ESA) with appropriately engineered excited-state dynamics, thereby enabling efficient NLA over a 500 nm bandwidth in the NIR for pulsewidths ranging from 75 fs to 40 ns. These characteristics give rise to temporally agile, broadband optical limiting for solutions of this material in bulk cells. Finally, introduction of the material in a waveguide device geometry results in further enhancement of the optical limiting response over the bulk geometry.

2. Metalloporphyrin polymers

Bis(ethynyl)porphyrin polymers exhibit strong electronic coupling between adjacent macrocycles via butadiynyl linkages [11] and it is this coupling that underlies both the effective charge transport in these molecular wires [12] as well as the cooperative enhancement of γ, the microscopic third-order nonlinearity, with increasing chain length for oligomeric porphyrins [13]. The latter observation has spurred a large expanse of current research devoted to investigating the nonlinear optical properties of linked porphyrins [14-16]. The electronic coupling of the porphyrins is responsible for the strong 2PA response ($\delta = 6400 \times 10^{-50}$ cm^4 s photon^{-1} per macrocycle) of single-stranded zinc-based porphyrin polymers at 980 nm [17], however the response at wavelengths greater than 1060 nm is reduced considerably ($\delta < 450 \times 10^{-50}$ cm^4 s photon^{-1} per macrocycle). The coupling should also lead to augmented ESA. However, it has been observed in ethynyl [18] and bis-ethynyl [19] linked zinc-porphyrin oligomers that an increased number of macrocycles leads to a decreased triplet-state yield and concomitant sub-ns excited-state lifetimes, which would result in limited optical limiting temporal dynamic range. To overcome these issues of non-optimal excited-state dynamics and moderate 2PA response, we have investigated a heavy atom (lead) containing porphyrin polymer, which has shown an enhanced value of γ (by nearly ten times) at a single wavelength (1064 nm) compared to its zinc-based counterpart [20] suggesting increased 2PA activity. Furthermore, the inclusion of lead in the macrocycle should promote an enhanced intersystem crossing, increasing the population in the lowest lying triplet state and leading to more effective optical limiting for longer pulses [21]. The structure of the lead bis(ethynyl)porphyrin polymer investigated here is shown in Fig. 1c, inset (for synthetic details see Ref. [20]) and consists of ~13 repeat units. Its absorption spectrum in solution possesses a strong and sharp absorption band (Q-band) that peaks at 858 nm. This characteristic, in conjunction with the solubilizing aryl substituents on the meso-positions of the porphyrins, permits concentrated solutions to be used with minimal linear loss in the NIR above 1000 nm. Furthermore, these bulky, flexible sidechains, combined with the modest

#115474 - $15.00 USD Received 10 Aug 2009; revised 23 Sep 2009; accepted 24 Sep 2009; published 29 Sep 2009

chain length, prevent significant aggregation from being observed up to 1×10^{-2} M concentrations (as evidenced by the independence of the absorption spectra on concentration).

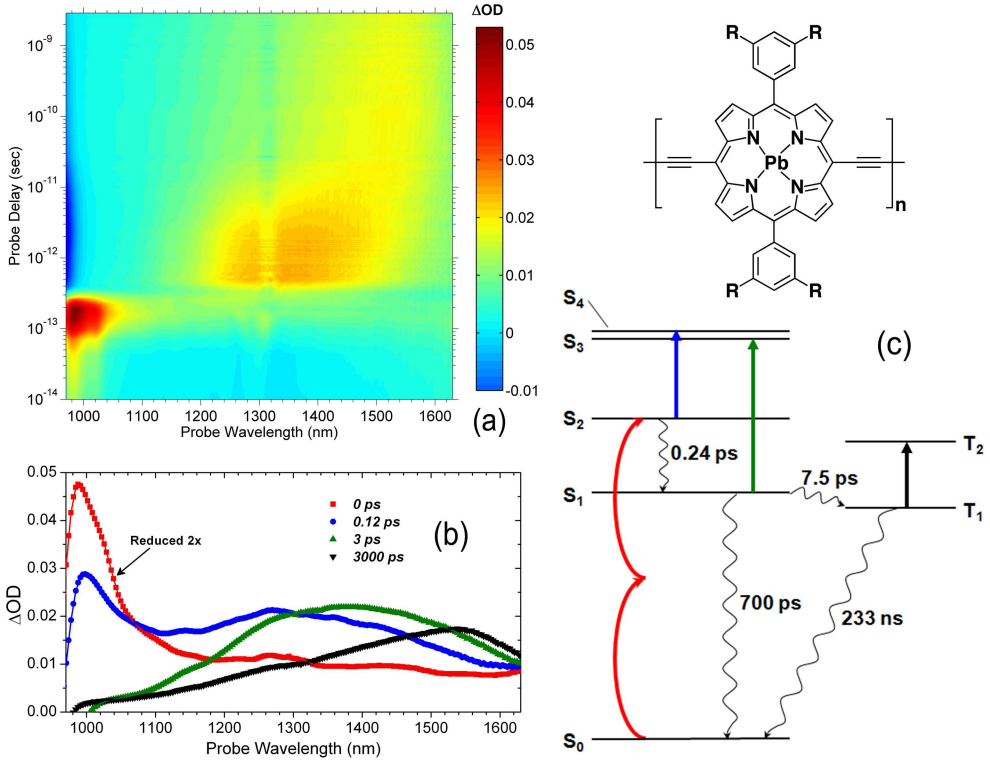

Fig. 1. Femtosecond transient absorption (TA) kinetics/spectra and state-level diagram for the porphyrin polymer. a, Time-wavelength representation of fs-TA following 2PA (λ_{exc} = 1300 nm) into S_2 and b, representative transient spectra at various probe delays. Residual scattered light from the excitation beam is evident and early time spectra have been reduced in amplitude for ease of viewing. c, energy level diagram and decay lifetimes determined from TA data. Upper-state lifetime decays were assumed to be fast ($\tau < 0.1$ ps). Inset (above) shows the chemical structure of the lead-based bis(ethynyl)porphyrin polymer with R = $CON(CH_2CHEtBu)_2$.

3. Experimental methods

3.1 Nonlinear spectroscopic techniques

In order to characterize the relevant NLA properties and dynamics of the lead bis(ethynyl)porphyrin polymer, we performed fs and ns pump-probe transient absorption (TA) spectroscopy. For these experiments, the porphyrin polymer was prepared in solutions of chloroform with 10% pyridine (both spectroscopic grade, Sigma-Aldrich) in ~1 × 10^{-4} M concentrations (all concentrations are given on a per macrocycle basis) for 1PA pumping and ~4 × 10^{-3} M for 2PA pumping. fs-TA was performed using a commercially available pump-probe spectroscopy system (Helios, Ultrafast Systems). A portion (~5%) of a 1 kHz repetition rate Ti:Sapphire regenerative amplifier (Spitfire, Spectra-Physics) operating at 800 nm provided the probe pulse to generate white-light continuum (WLC, 850 – 1650 nm) while the remainder generated the pump pulse (tunable from 465 – 2900 nm, ~75 fs HW1/e) following passage through an optical parametric amplifier (TOPAS-White, Spectra-Physics). The pump beam was chopped at 500 Hz to obtain both pumped (signal) and non-pumped (reference) probe spectra sequentially for generation of a ΔOD spectrum at each temporal

#115474 - $15.00 USD Received 10 Aug 2009; revised 23 Sep 2009; accepted 24 Sep 2009; published 29 Sep 2009

delay (averaged for 1.5 seconds). The result was a wavelength-versus-time 2-D array of ΔOD values. The sizes of the pump and probe beams at focus were measured (for the numerical fitting procedure, see below) using a knife-edge scan. Using a solution of carbon tetrachloride, both the instrument response function (~200 fs) and a correction factor to account for the chirp of the WLC probe (applied to all data sets) were determined. The solutions were studied in 2 mm path-length quartz cuvettes and were stirred continuously throughout the data acquisition. The stability of the transient signals during the experiment and unchanged linear absorption spectra observed immediately following the TA runs showed that no appreciable photodegradation had occurred.

For ns-TA, the pump (tunable from 410 – 2000 nm, ~4 ns HW1/e) was from an optical parametric oscillator (MOPO-PO, Spectra-Physics) driven by a 10 Hz repetition rate, high-energy Q-switched Nd:YAG laser (Quanta-Ray PRO-250-10, Spectra-Physics) operating at 355 nm. The white light probe (long pass filter used, >850 nm) was produced by a 240 W tungsten-halogen bulb controlled by a radiometric power supply (Oriel 69931, Newport Corporation). After passing through the sample at a small angle with respect to the pump, the probe beam was coupled into a monochromator (SP-2150i, Princeton Instruments) and was detected at the exit slit by a high-speed InGaAs PIN photodiode (HCA-S-200M-IN, Femto). The detector was connected to an oscilloscope (TDS3024, Tektronix) and the probe signal was synchronously triggered with the pump pulse. The data were averaged over ~5000 shots, transferred to a PC and manipulated to generate a ΔOD versus time curve. Global fitting of these transients for different probe wavelengths allowed for reconstruction of the triplet ($T_1 \rightarrow T_2$) spectrum that showed good correlation with the long delay (3000 ps) fs-TA spectrum in Fig. 1b. Solutions were contained in 1 cm path-length quartz cuvettes and were stirred continuously. Again, photodegradation effects were minimal. Deoxygenated solutions (via freeze-pump-thaw method) showed 233 ns lifetimes while air-saturated solutions showed 91 ns lifetimes.

Femtosecond-pulsed open aperture Z-scan experiments were performed to determine the magnitudes of the ultrafast optical nonlinearities (see below). The details for these experiments have been described previously elsewhere [22].

3.2 Optical limiting

The laser sources used for fs- and ns-pulsed optical limiting were the same as those used for the TA experiments described above with the exception that the repetition rates were reduced (1 kHz to 50 Hz for fs, 10 Hz to 1 Hz for ns) to eliminate spurious cumulative effects associated with thermally-induced nonlinearities. Detection of the energies both before and after the sample was accomplished using large area Germanium photoreceivers (2033, New Focus). These signals were passed through Boxcar integrator units (SR250, Stanford Research Systems) and the processed signals were acquired using a data acquisition card (6025E, National Instruments) and a home-built Labview program. The input energies were varied using computer-controlled half-waveplate rotators (PR50-PP, Newport Corporation) in conjunction with polarizers.

For bulk optical limiting, porphyrin polymer solutions (chloroform with 10% pyridine, 0.3 – 1.0×10^{-2} M) were used in 1 mm glass cuvettes. The focusing geometries were ~F/5 for ns pulses and ~F/20 for fs pulses and the foci were placed in the middle of the cuvette's pathlength. The beam sizes around focus (~20 um HW1/e^2) were measured using pinhole and knife-edge scans and were determined to be Gaussian in shape. The collection geometries (~F/2) assured total collection of the exiting beam. For microcapillary (MC)-based optical limiting, the porphyrin polymer solutions (0.3 – 1.0×10^{-3} M) were dissolved in chlorobenzene:10% pyridine to possess an appropriate refractive index for multimodal coupling. During the optical limiting studies, a stainless-steel liquid-tight sample holder held both the solution-filled MCs and a reservoir of additional solution to prevent solvent evaporation and to allow for efficient optical coupling. Solution-filled MCs (Polymicro

#115474 - $15.00 USD Received 10 Aug 2009; revised 23 Sep 2009; accepted 24 Sep 2009; published 29 Sep 2009

Technologies) possessed a NA ≈ 0.4, so efficient coupling (> 80%) was achieved with a 10× objective (NA = 0.25) and collection was accomplished with a 20× objective (NA = 0. 5). The beam size inside the MC was determined by imaging its back face onto a Vidicon camera (MicronViewer 7290a, Electrophysics).

3.3 Nonlinear beam propagation

A numerical method for nonlinear beam propagation was implemented to both simulate optical limiting experiments and to fit fs-TA and open aperture Z-scan data to extract the pertinent optical nonlinearities. Beam propagation through a nonlinear medium can be numerically modeled by simultaneously solving both the population rate equations and the propagation equation (see for example Ref. [23]). The excitation (pump) beam/pulse was assumed to be Gaussian in space/time and its shape was allowed to change during propagation through the sample, either due to linear (i.e. focusing, linear absorption) or nonlinear propagation effects (i.e. attenuation due to nonlinear absorption). Consequently, the set of differential rate equations associated with the energy level diagram (Fig. 1a) were time-dependent and were numerically solved using the Runge-Kutta method which provided stable and well-converged solutions. Following propagation through the sample, which was divided into smaller propagation slices for greater accuracy, the excitation beam/pulse was integrated over space/time to get the overall energy transmittance. For simulating Z-scan or optical limiting data, the beam propagation routine merely needed to be repeated for a series of axial focus positions or input energies, respectively. To simulate TA, an additional beam/pulse (probe) was overlapped with the pump and the probe energy transmittance was determined for each temporal delay between the two pulses.

4. Nonlinear spectroscopy

TA spectroscopy on the lead bis(ethynyl)porphyrin polymer was performed following excitation by 1PA into the lowest lying one-photon allowed state ($S_0 \rightarrow S_1$, λ = 850 nm) or by 2PA into the lowest lying two-photon allowed state ($S_0 \rightarrow S_2$, λ = 1300 nm). Representative kinetics and spectra following excitation into S_2 are shown in Figs. 1a and 1b. A state level diagram (Fig. 1c) with the associated decay lifetimes was constructed from a global analysis of the TA data (singlet decays were extracted from fs-TA data and the triplet decay from the ns-TA data) and consists of a five-level singlet manifold and two-level triplet manifold. The ultrafast components (τ_{delay} < 0.3 ps) of the decay kinetics in Fig. 1a are dominated by a component due to 2PA (instrument-response limited) and by ESA associated with the $S_2 \rightarrow S_4$ transition. The remaining kinetics consist of $S_1 \rightarrow S_3$ ESA rapidly giving way to triplet ESA ($T_1 \rightarrow T_2$). The short intersystem crossing lifetime results in a near-unity triplet yield ($\phi_T \approx$ 0.99) as a consequence of the heavy-atom effect, which is consistent with the observations of Duncan et al. [24] upon appending heavy-metal containing (Ru or Os) terminal macrocycles onto porphyrin oligomers.

Strong broadband ESA, for the lead porphyrin polymer, is observed over a wide temporal range due to contributions from the excited singlet and triplet states. The transient spectra at specific delays in Fig. 1b provide a good representation of the true ESA spectra (transition, λ_{max}, full width at half maximum): [$S_2 \rightarrow S_4$, 1270 nm, ~2800 cm^{-1}], [$S_1 \rightarrow S_3$, 1380 nm, ~2260 cm^{-1}], and [$T_1 \rightarrow T_2$, 1545 nm, ~2040 cm^{-1}]. The singlet transitions are extremely broad, attributable to pronounced conformational heterogeneity in the excited-state [18], and are similar in width to the NIR transitions found for ethynyl-linked zinc-porphyrin oligomers [18], albeit slightly broader for the lead polymer. The broad triplet ESA transition exhibits a similar spectral width to the heavy-metal terminated porphyrin oligomers [24] but is red-shifted by nearly 400 nm. The differences in the ESA characteristics from the porphyrin oligomers may be partly attributable to the longer conjugation pathway in the lead polymer. It is important to note that the different decay kinetics of each transition allows each ESA

#115474 - $15.00 USD Received 10 Aug 2009; revised 23 Sep 2009; accepted 24 Sep 2009; published 29 Sep 2009

process to play a critical role in the efficacy of the system for optical limiting in different temporal pulse regimes: $S_2 \rightarrow S_4$ for fs, $S_1 \rightarrow S_3$ for ps, and $T_1 \rightarrow T_2$ for ns timescales. Finally, the spectrum at τ_{delay} = 0 ps is predominantly due to 2PA. The 2PA spectrum exhibits a broadband response like ESA, but is spectrally complimentary since it monotonically increases in magnitude towards shorter wavelengths making the combined nonlinear response for 2PA-ESA spectrally constant.

Table 1. ESA and 2PA cross-sections in near infrared for the lead bis(ethynyl)porphyrin polymer.[a]

	1064 nm	1150 nm	1300 nm	1450 nm	1550 nm
δ [GM]	14000[b]	6800	5200	1200	650
σ_{24}^{S} [m^2]	1.3×10^{-20}	5.1×10^{-20}	5.3×10^{-20}	4.0×10^{-20}	3.8×10^{-20}
σ_{13}^{S} [m^2]	0.7×10^{-20}	2.8×10^{-20}	6.2×10^{-20}	5.3×10^{-20}	3.2×10^{-20}
σ_{12}^{T} [m^2]	0.6×10^{-20}	1.3×10^{-20}	2.2×10^{-20}	3.9×10^{-20}	3.8×10^{-20}

[a] These values are given on a per macrocycle basis. Errors associated with values were determined to be ±15%. Note: 1 GM = 1 x 10^{-50} cm^4 s photon^{-1}.

[b] This value is approximately three times smaller than the value given in Ref. [20] from degenerate four-wave mixing. While this discrepancy is not large, it cannot be ascribed to experimental error alone. ESA could contribute to an overestimation of δ in Ref. [20], particularly since ps excitation was used.

Given the presence of multiple ESA bands with significant spectral overlap, a standard ratiometric method involving ground-state bleaching [25] of the polymer could not be used to determine the absolute absorption cross-sections. Instead, a nonlinear beam propagation routine was utilized to fit the experimental data and extract the appropriate nonlinearities. By utilizing experimentally determined beam profile and pulse shape parameters, as well as the state decay lifetimes shown in Fig. 1c, the optical nonlinearities became the only unknown parameters thereby ensuring the fitting process was not underspecified. ESA cross-sections for the $S_1 \rightarrow S_3$ (σ_{13}^{S}) and $T_1 \rightarrow T_2$ (σ_{12}^{T}) transitions were determined by fitting the 1PA fs-TA kinetics. In order to determine σ_{24}^{S} (associated with $S_2 \rightarrow S_4$ transition) and the 2PA cross-sections (δ), fs-pulsed open-aperture Z-scans were performed and the data were fit using the numerical routine. Absolute cross-section values were determined at five representative wavelengths throughout the NIR and are shown in Table 1. The extracted nonlinearities follow the transient spectra in Fig. 1b and confirm both the broad spectral bandwidths and how the 2PA and ESA processes are spectrally complimentary. The values for δ are some of the largest found in this spectral region [14-16] and follow the general spectral trends observed for porphyrin-based single macrocycles [26], directly linked dimers [16], and butadiyne-linked oligomers [17]. The ESA cross-sections are quite large (exceeding even the peak ground-state cross-section, $\sigma_{01}^{S} \approx 2\times10^{-20}$ m^2 at 858 nm), suggesting significant delocalization of both the singlet and triplet wave-functions as a consequence of the strong electronic coupling between adjacent macrocycles. These values compare favorably (molar extinction coefficients, ε, from ~20,000 M^{-1} cm^{-1} to ~160,000 M^{-1} cm^{-1}) with the ethynyl-linked [18] or heavy-metal macrocycle terminated [24] zinc-based porphyrin oligomers, and exceed even some of the largest ESA cross-sections found in the visible portion of the spectrum [3].

#115474 - $15.00 USD Received 10 Aug 2009; revised 23 Sep 2009; accepted 24 Sep 2009; published 29 Sep 2009

5. Optical limiting

To determine the optical limiting capabilities of the lead-based porphyrin polymer, experiments were performed using fs- and ns-pulsed excitation on solutions at three representative wavelengths effectively covering the NIR spectral region. The results are shown in Fig. 2. As desired for optical limiting, the linear transmittances of the samples are quite high ($T_L \geq 89\%$ for all wavelengths). Attenuation due to nonlinear absorption begins at reasonably low input energies (> ~50 nJ for fs pulses, > ~1 μJ for ns pulses). For higher input energies, clamping of the output energies is observed (Fig. 2, insets). The optical suppression for each system, defined as $1/T_{NL}$ (where T_{NL} is the sample transmittance at either the highest achievable input energy or the energy immediately prior to cuvette damage, whichever is reached first), was substantive throughout the NIR and exceeded 18 dB (60×) in the fs-pulse regime and 14 dB (25×) in the ns-pulse regime.

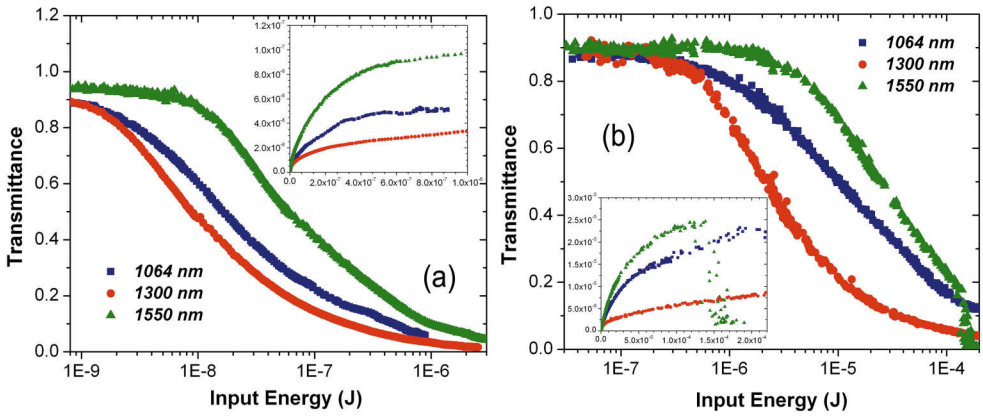

Fig. 2. Broadband optical limiting of the porphyrin polymer solutions. a, fs-pulsed (75 fs, HW1/e) optical limiting and b, ns-pulsed (4 ns, HW1/e) optical limiting on solutions of porphyrin polymer in 1 mm cuvettes at various wavelengths in NIR spectral region. Experimental parameters are given in the Experimental methods section. Insets show output energy versus input energy illustrating a clamping effect at higher energies. Optical damage of the cuvette is evident for ns-pulsed optical limiting data (1550 nm) around an input energy of ~140 μJ.

While these observations clearly illustrate the broad spectral and temporal optical limiting capabilities of the lead bis(ethynyl)porphyrin polymer in solution, simulations based on the numerical nonlinear beam propagation routine were undertaken to further illustrate the exceptional optical limiting capabilities. The simulations utilized only experimentally determined values and are shown in Figs. 3a and 3b. The curves show strong correlation with the experimental data despite the absence of any additional fitting parameters and therefore lend credence to the dominant nonlinear absorption process being 2PA-ESA. It should be noted that, for shorter excitation wavelengths (< 1300 nm) in the ns-pulsed optical limiting data (Fig. 2b), the energies at which attenuation due to nonlinear absorption begins were slightly lower than predicted by a pure 2PA-ESA process. By allowing a fraction of the ground-state population (< 10%) to be promoted by 1PA for these wavelengths, this earlier turn-on was able to be successfully simulated, however it only plays a significant role for longer duration pulses. Given the wide range of chain lengths (and mixture of conformations found each chain length) for such bis(ethynyl)porphyrin polymers [20], there is inhomogenous broadening of the tail of the absorption bands and therefore weak 1PA extending far beyond the peak absorption maximum (λ = 858 nm). Using the same excitation conditions as those described above, simulations at 1150 nm and 1450 nm were run and the optical limiting response was similar to the other excitation wavelengths, consistent with the

#115474 - $15.00 USD Received 10 Aug 2009; revised 23 Sep 2009; accepted 24 Sep 2009; published 29 Sep 2009

broadband nonlinear absorption discussed above. To investigate the temporal dynamic range of optical limiting with this system, simulations were run for different excitation wavelengths utilizing pulses of 10 ps in duration (Fig. 3c) as well as at a particular wavelength, 1300 nm, for a number of different excitation pulsewidths ranging from 75 fs to 40 ns (Fig. 3d). The optical limiting simulations reveal strong optical suppression over the entire temporal excitation range. This is a consequence of the favorable excited-state kinetics that permit different ESA transitions to play key roles for different pulsewidths during the optical limiting process.

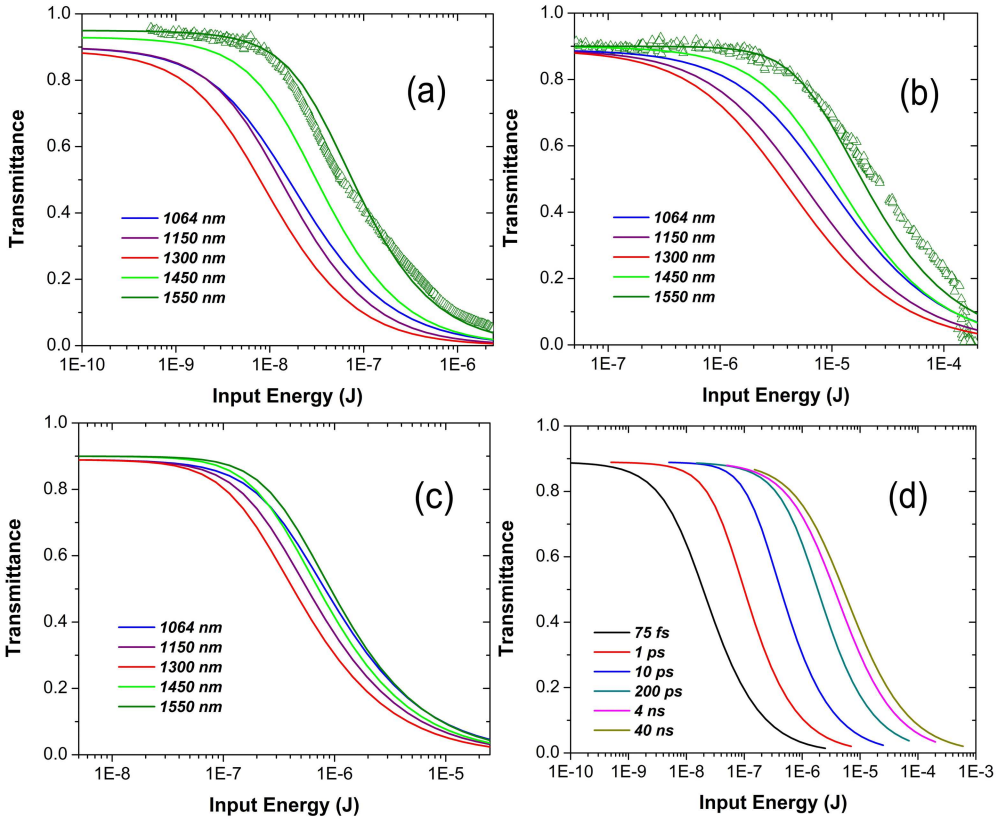

Fig. 3. Optical limiting simulations of the porphyrin polymer solutions. Numerical simulations based on nonlinear beam propagation through solutions of the porphyrin polymer in 1 mm cuvettes. Optical limiting at various wavelengths for different pulsewidths (HW1/e): a, 75 fs; b, 4 ns; c, 10 ps. d, optical limiting at 1300 nm for various excitation pulsewidths (HW1/e). Additionally, experimental data for fs-OL and ns-OL at 1550 nm from Figs. 2a and 2b are overlaid in Figs. 3a and 3b, respectively, for comparison. Photophysical and nonlinear optical parameters for the optical limiting simulations are taken from Figure 1c and Table 1, respectively. Experimental parameters are taken from Figure 2 for simulations in Figs. 3a and 3b, and were assumed to be ~F/5 with a 20 um (HW1/e^2) beam size for Figs. 3c and 3d. For Figure 3d, the onset of nonlinear attenuation moves to higher energies for longer pulsewidths, consistent with the irradiance-dependence of the excitation process, 2PA. However, this is mitigated to a certain extent for longer pulses by the small amount of resonant excitation.

The optical device geometries employed for optical limiting with the lead bis(ethynyl)porphyrin polymer up to this point (i.e. relatively fast focusing optics and bulk liquid cells) have not been optimal. Microcapillary (MC) waveguide arrays filled with liquid nonlinear materials are a promising alternative since they can provide the functionalities of

#115474 - $15.00 USD Received 10 Aug 2009; revised 23 Sep 2009; accepted 24 Sep 2009; published 29 Sep 2009

both imaging as well as optical limiting [27, 28]. The key benefit involves the effective confinement and propagation of the beam within the MC which provides an extended nonlinear interaction length that can greatly exceed that of a F/5 lens focusing in a bulk sample. optical limiting using MC waveguides in the visible spectral region has been observed for nonlinear processes such as 1PA-ESA [29], 2PA [4], and thermal refraction [30]. Furthermore, single MCs have often been employed to avoid effects due to potential crosstalk with neighboring waveguides [4, 29], making analysis of the nonlinear absorption inside the MC more straightforward. Accordingly, fused silica MCs ($n_{cladding}$ = 1.444, diameters of 20 – 30 μm, lengths of 1.8 cm) were filled with chlorobenzene solutions of the porphyrin polymer ($n_{core} \approx 1.51$), which resulted in nonlinear multimode waveguides. Efficient coupling of ns-pulsed excitation in the NIR resulted in effective beam diameters (~12 – 13 μm) inside the waveguides, significantly smaller than the diameter of the actual MCs. This is consistent with previous observations [29] that only a subset of the possible modes in the guide are actually excited during propagation. The results for the MC-based optical limiting with ns pulses are shown in Fig. 4. The curves are comparable to the bulk ns-pulsed optical limiting data shown in Figure 2b with similarly high linear transmittances ($T_L \approx 80\%$) and slightly

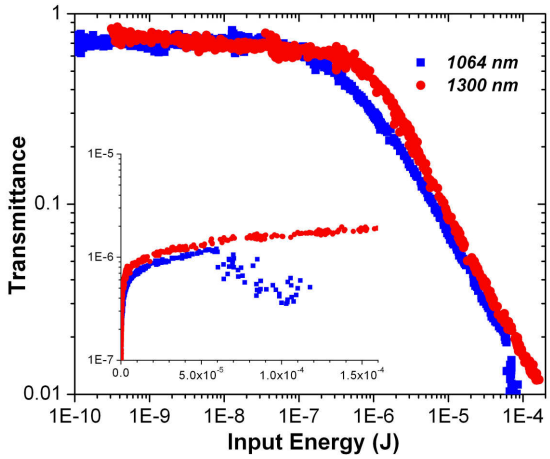

Fig. 4. Optical limiting in microcapillary waveguides for porphyrin polymer solutions. ns-pulsed (4 ns, HW1/e) optical limiting of porphyrin polymer solutions in 1.8 cm microcapillaries of 20 – 30 μm in diameter. Experimental parameters are given in the Experimental methods section and insets show output energy versus input energy. Generation of a bubble in the MC resulted in strong scattering around 70 μJ for the 1064 nm data.

lower turn-on energies (~0.3 μJ). However, the nonlinear suppressions for the MC-based optical limiting data are more pronounced: 17 dB (50×) for 1064 nm and nearly 20 dB (100×) for 1300 nm. The benefit of the increased nonlinear interaction length provided by the MC waveguides is that these pronounced suppressions occur *despite* an order-of-magnitude decrease in polymer solution concentration compared to the bulk optical limiting experiments. This is critical since concentration, or ground-state population density, is a factor controlling the effective pumping rate of species available for 2PA-ESA and its increase would only serve to further augment the nonlinear suppression. Use of smaller diameter MCs should also improve the efficacy of optical limiting. Finally, the same broad spectral and temporal coverage observed for the bulk optical limiting experiments should be immediately translatable to the nonlinear waveguide geometries. It should also be noted that at these concentrations, similar polymers have been doped into PMMA host polymers to form solid

#115474 - $15.00 USD Received 10 Aug 2009; revised 23 Sep 2009; accepted 24 Sep 2009; published 29 Sep 2009

films [31] suggesting that these current porphyrin polymers should be suitable for solid-state waveguide applications as well.

6. Conclusions

We have shown that a lead bis(ethynyl)porphyrin polymer can effect optical limiting over a range of about 500 nm in the NIR (ca. 1050 – 1600 nm) and for laser pulsewidths spanning five orders-of-magnitude from 75 fs to 40 ns. Nonlinear spectroscopic studies reveal the unprecedented spectral/temporal coverage to be a consequence of the broad, overlapping two-photon and excited-state absorption bands, the magnitude of the nonlinear response, and the corresponding excited singlet and triplet state dynamics, which should provide a rational design strategy for improved optical limiting in the future. Finally, the properties of this metalloporphyrin polymer material has enabled the demonstration of strong pulse attenuation in device experiments. A single material that can provide such broadband optical limiting over a large temporal dynamic range could prove to be extremely valuable for protection of sensors, dynamic noise suppression, or optical signal regeneration.

Acknowledgements

This material is based upon work supported in part by the STC Program of the National Science Foundation under Agreement Number DMR-0120967 and the DARPA MORPH Program and ONR (N00014-04-0095 and N00014-06-1-0897). We gratefully acknowledge Steven Flom (Naval Research Laboratory) for providing the design schematic for the sample holder used to house the microcapillary waveguides during the MC-based optical limiting studies.

#115474 - $15.00 USD Received 10 Aug 2009; revised 23 Sep 2009; accepted 24 Sep 2009; published 29 Sep 2009